THE GENERATION OF NOISE BY THE FLUCTUATIONS IN GAS TEMPERATURE INTO A TURBINE.

N.A. Cumpsty and F.E. Marble

CUED/A TURBO/TR 57 (1974)

THE GENERATION OF NOISE BY THE FLUCTUATIONS IN GAS TEMPERATURE INTO A TURBINE

SUMMARY

An actuator disc analysis is used to calculate the pressure fluctuations produced by the convection of temperature fluctuations (entropy waves) into one or more rows of blades. The perturbations in pressure and temperature must be small, but the mean flow deflection and acceleration are generally large. The calculations indicate that the small temperature fluctuations produced by combustion chambers are sufficient to produce large amounts of acoustic power.

Although designed primarily to calculate the effect of entropy waves, the method is more general and is able to predict the pressure and vorticity waves generated by upstream or downstream going pressure waves or by vorticity waves impinging on blade rows.

1. INTRODUCTION

It is now widely accepted that jet propulsion engines frequently produce a significantly higher level of noise from their exhaust than the prediction of jet noise theory, particularly if the jet velocity is low. Experimental tests using carefully designed test rigs, however, are able to show the v^8 dependence of sound pressure level on jet velocity down to velocities of the order of 100 m/s or less. Some of this extra noise, often referred to as excess or tailpipe noise, has been successfully correlated with incidence onto struts in the jet-pipe and some is attributable to the tones from the turbine. There remains, nevertheless, a residual discrepancy between engine results on the one hand and the theory and laboratory model measurements on the other. This residual appears to be random in character and to have a frequency spectrum which may be almost identical to pure-jet noise. Circumstantial evidence clearly links this extra noise with the combustion process in engines, and the present paper develops a simple theory which explains how combustion in engines can give rise to noise.

The assumption underlying the model is that there are significant fluctuations in the temperature of the gas stream leaving a combustion chamber. A recent paper by Dils[1] has shown that the standard deviation of the temperature leaving the combustion chamber of a modern engine approaches 10% of the mean absolute temperature, although this appears to be an overestimate and 2% seems more realistic. It was also found that spectrum of these fluctuations extends up to at least 300 Hz, beyond this frequency the response of the instrument used in the study reported by Dils dropped rapidly. In the present model temperature fluctuations entering a turbine blade row give rise to pressure waves which may be transmitted down the jet pipe and radiated as noise. The temperature fluctuations entering the blades are convected by the flow and have no pressure or velocity perturbations associated with them, but are in fact entropy waves, where the entropy perturbation is $s' = C_p T'/T$. It is useful to refer to them as entropy waves to distinguish the variation in temperature associated with these convected waves from the temperature variation due to the isentropic

process in a pressure wave.

The model used has origins elsewhere. The same approach was used to find the reflection upstream from rocket nozzles by Tsien and more recently Candel[2] has analysed the effect of entropy waves into a choked convergent-divergent nozzle. The salient features of the present model together with some of the ramifications are as follows:

(a) The blade passages are assumed sufficiently short that the flow inside them may be treated as if it were steady, so that disturbances on both sides of the blade row are in phase. This allows the precise blade details to be ignored, and the upstream and downstream perturbations are matched across the row. For frequencies below about 1kHz (for which the acoustic wavelength at the turbine inlet will be about ¾m) this assumption will be very good even for large engines, except for Mach numbers very close to one.

(b) The blade pitch is assumed infinitesimal. This means that no information can be generated close to the blade passing frequency, but this is believed to be very much greater than the frequency of significant entropy fluctuations. This assumption allows rotor rows to be treated in just the same way as stators after allowing for the change in the mean flow Mach number and direction relative to the rotor. Assumptions (a) and (b) characterise what follows as an "actuator disc" type of solution.

(c) Although the incident entropy perturbations are required to be small, the deflection and acceleration of the mean flow in the blades will normally be large and the pressure and entropy perturbations are of the same order. This appears to be a very good representation of the disturbances occurring in real turbines.

(d) In the analysis the input disturbance is assumed to be harmonic, but because the analysis is linear it can be immediately generalised to a random input.

(e) The axial velocity is taken to be everywhere subsonic.

(f) The flow is treated as two-dimensional so that radial variations are neglected.

(g) Although the length of the blades is assumed small the effect of the axial distance between blade rows on the phase and

amplitude is explicitly included.

This work set out to calculate the pressure wave amplitudes produced by a succession of blade rows in response to a small amplitude entropy fluctuation. It turns out that the method is more general than this and can find the pressure or vorticity amplitude due to incident pressure or vorticity waves as well. Indeed this is necessary once more than one isolated blade row is to be considered because each blade row produces pressure and vorticity waves which in turn affect the others.

Four perturbations are considered, upstream and downstream going pressure waves, vorticity waves and entropy waves. Four equations are needed for a solution. One, the conservation of entropy, is mathematically trivial but means that entropy is not produced by any of the other perturbations. Conservation of mass flow and energy are also applied. The fourth equation depends on the flow conditions at outlet; for a subsonic outlet flow the Kutta condition is applied at the blade trailing edge, whilst for supersonic outlet flow a constant corrected mass flow is assumed upstream of the blade row.

In the next section the kinematic behaviour of the waves systems is developed and following this, in Section 3, the equations to be applied across each blade are described in more detail. The method of solution is outlined in Section 4. Because in many cases the acoustic power is likely to be of most interest the method of calculating this from the amplitude of the pressure wave is explained in Section 5. Finally, Section 6 descibes some calculations performed and discusses the results.

2. KINEMATIC CONSIDERATIONS

The movement of vorticity and entropy waves on the one hand and pressure waves on the other is quite different. Whereas vorticity and entropy are convected by the mean flow, the pressure waves propagate relative to the moving flow. It is necessary here to develop the kinematics for the two types of propagation. The input is assumed throughout to be a disturbance of radian frequency ω with a wavelength in the circumferential (cascade) direction of Y. The notation and geometry considered are shown in Figure 1.

In calculating the response of a blade row it is necessary to consider the fluid velocities sensed in a frame of reference fixed relative to the blades. The directions of the velocity perturbations associated with pressure or vorticity waves are, of course, unaffected by a change in frame of reference. The change of frame of reference normally involves a change of frequency but, in the actuator disc assumption, the response of the blades is independent of frequency so that this can be neglected. Because of this all the wave properties can be evaluated in a stationary frame of reference.

(a) Entropy wave

The entropy variation is assumed to vary sinusoidally with radian frequency ω and to form standing waves along the cascade (in the y direction) of length Y. This is an idealised description of "hot spots" convected into the turbine. The frequency, f, is equal to the axial velocity divided by the axial length of the "hot-spot". At a reference plane ($x = 0$) the form of the perturbation is

$$s' = \hat{s}' e^{i\omega t} \cos 2\pi y/Y \qquad (1)$$

where the symbol $\hat{}$ denotes the amplitude of the perturbation. The solution is analytically much easier if the standing wave pattern is resolved into two travelling waves and each wave system is treated independently, so that

$$s' = \frac{\hat{s}'}{2} e^{i\omega t}\left(e^{i2\pi y/Y} + e^{-i2\pi y/Y}\right) \qquad (2)$$

This is mathematically identical to equation 1, the positive exponent corresponds to a disturbance moving to the right (negative y direction) and the negative exponent to disturbances of equal magnitude moving to the left (Figure 1). It is convenient to contract equation 2 to

$$s' = \frac{\hat{s}'}{2} e^{i\omega t} e^{\pm i2\pi y/Y}$$

where ± implies that the sum of two exponentials should be taken.

The entropy waves are convected by a mean flow having components U and V in the positive x and y direction respectively.

The form of the entropy waves away from the $x=0$ plane is therefore:

$$s' = \hat{s}' \, e^{i\omega(t-\frac{x}{U})} \, e^{\pm i2\pi(y - xV/U)/Y} \tag{3}$$

(b) Vorticity waves

The form of the harmonic variation in these waves is identical to that of the entropy waves given by equation 3. Thus

$$v' = \hat{v}'_{\pm} \, e^{i\omega(t-\frac{x}{U})} \, e^{\pm i2\pi(y - xV/U)/Y} \tag{4}$$

There may be a phase shift in the vorticity relative to the entropy and this is equivalent allowing the amplitude to be complex. In addition the amplitude will not in general be equal for waves to the right and left, and $\hat{v}_{\pm}$ is used to denote this.

The lines of constant phase (i.e. the wave fronts) may be obtained from equation (4) by equating the x and y terms in the exponents to zero

$$-\frac{\omega x}{U} \pm \frac{2\pi}{Y}\left(y - \frac{xV}{U}\right) = 0$$

Rearranging

$$y/x = \frac{\pm\frac{\omega Y}{2\pi} \pm V}{U} = \tan\beta \tag{5}$$

where β is the angle between the axial direction and the line of constant phase, which is, of course, different for the waves to the right (+ sign) and waves to the left (-ve) sign.

Each blade will shed vorticity, but because of the actuator disc assumption the distance between each blade and between each vortex is infinitesimal. A line of constant phase therefore represents a line through an infinite array of vortices of equal amplitude and the same sign. In other words the line of constant phase is a vortex sheet along which the perturbation consists of a shearing action. The velocity perturbation associated with the vorticity is therefore parallel to the wave fronts and inclined at β to the axial direction.

(c) The Pressure waves

In general there are four sets of pressure waves in any region, a pair to the right and to the left, with one of each pair propagating upstream and the other downstream. These waves propagate relative to the moving flow as well as being convected by it.

The general form of the pressure wave can be written

$$p' = \hat{p}' e^{i\omega t} e^{\pm i 2\pi y/Y} e^{ikx}, \qquad (6)$$

the amplitude, $\hat{p}'$, is in general different for each wave direction. The variation with respect to both time and the y-direction are assumed to be imposed by the input wave, but the form of the x variation has to be found from a solution to the wave equation. For a two dimensional geometry (using the method of separation of variables) the axial wave number, k, can be shown to be

$$k = \frac{-2\pi/Y}{1-M_x^2}\left(M_x\left(\frac{\omega Y}{2\pi a} \pm M_y\right) \pm \sqrt{\left(\frac{\omega Y}{2\pi a} \pm M_y\right)^2 - (1-M_x^2)}\right) \qquad (7)$$

M_x and M_y are the Mach numbers of the axial and tangential mean velocities. The positive sign in front of M_y is applicable for waves propagating to the right (negative y-direction) and the positive sign in front of the square root is for waves propagating upstream (negative x direction). The argument $(\omega Y/2\pi a \pm M_y)$ can be identified as the Mach number corresponding to the circumferential phase velocity relative to the moving gas.

When the argument inside the square root of equation 7 is positive the axial wave number is real, but whenever the argument becomes negative the wave number contains an imaginary component and the wave is attentuated in the x direction. Because the attenuation may be very rapid waves are usually described as "cut-off" whenever k is complex, Tyler and Sofrin[3]. Thus

$$p' = \hat{p}' e^{i\omega t} e^{\pm i 2\pi y/Y} e^{ik_R x} e^{-k_I x} \qquad (8)$$

In the analysis of blade row response which follows the velocity perturbation associated with the pressure waves is required. The relationship between pressure and velocity can be obtained by substituting equation 8 for pressure into the linearised equations of motion (see appendix). The axial and tangential perturbation velocities are related to the pressure by

$$\frac{w_x'}{a} = A_x \frac{p'}{\gamma p}$$

and

$$\frac{w_y'}{a} = A_y \frac{p'}{\gamma p}$$

If the wave is above cut-off A_x and A_y are real and are equal to $\cos\alpha$ and $\sin\alpha$, where α is angle the wave propagation velocity makes with the axial. Below cut-off A_x and A_y are complex and their form is given in the appendix by equation A6.

Three points about cut-off waves are worth mentioning. When waves are just at the point of cut-off the direction of the upstream and downstream waves is the same and is such that the axial component of the propagation velocity exactly equals the mean axial flow velocity. Furthermore, at the cut-off point the wave fronts are exactly normal to the constant phase lines of vorticity (or entropy). The direction of the velocity perturbation from the vorticity is therefore identical to the direction of the velocity perturbations from the pressure waves at the cut-off point.

Finally, it cannot be assumed that a wave system to the right or left which is cut-off in one region will be cut-off everywhere else. Cut-off is affected by mean flow velocities, particularly V, and by the reduction in the velocity of sound as the gas is expanded through the turbine. Moreover the small axial spacing between turbine blade rows means that very little attenuation of cut-off waves may occur. If the pressure waves are above cut-off downstream of the last blade row the behaviour is significant in regions which are cut-off.

3. THE BLADE ROW EQUATIONS

The governing equations were named in Section 2, and in this present section they will be developed and discussed in

more detail.

Although in some instances the input consists of a standing wave pattern in the circumferential (y) direction it is more convenient to treat it as two travelling wave systems to the left and right. Because the wave systems to the left and right are regarded as independent it is therefore possible to set up the equations in such a way that they apply to either set, and the behaviour of the left and right hand waves are then calculated in turn. In each region there are, in general, upstream and downstream propagating pressure waves, but in deriving the equations the pressure and velocity perturbation p' and w' are taken to represent the sum of the upstream and downstream waves. The direction of the velocity perturbation due to pressure is different for the upstream and downstream waves and it has to be understood that this difference will be allowed for where p' and w' are expanded.

In applying equations to the blade row the essential assumption is that the blade passage is sufficiently short that the conditions just upstream and downstream are in phase and may be related to one another as if they were steady. For the condition of interest here this assumption is almost always likely to be good for downstream going disturbances, but will fail for upstream going disturbances as the flow Mach number approaches one.

(a) Mass Continuity Equation

The continuity equation is $\rho_1 U_1 A_1 = \rho_2 U_2 A_2$ where conditions 1 and 2 refer to conditions just upstream and downstream of the blade row, ρ and U are the time mean density and axial velocity and A is the area. The continuity equation must still be satisfied if small perturbations ρ' and U' occur, so that

$$\frac{\rho_1'}{\rho_1} + \frac{U_1'}{U_1} = \frac{\rho_2'}{\rho_2} + \frac{U_2'}{U_2}$$

Assuming the gas to be at least semi-perfect the density perturbation ρ'/ρ can be expanded as $p'/p - T'/T$. Whereas the variation in pressure arises solely from the pressure waves, temperature fluctuations will be caused both by the entropy wave and by the pressure, so that $\frac{T'}{T} = \frac{s'}{c_p} + \frac{\gamma-1}{\gamma}\frac{p'}{p}$,

and the density variation can be written

$$\frac{\rho'}{\rho} = \frac{p'}{p} - \frac{s'}{c_p} - \frac{\gamma-1}{\gamma}\frac{p'}{p} = \frac{p'}{\gamma p} - \frac{s'}{c_p}$$

The velocity perturbation comes from the pressure and vorticity waves. In the continuity equation only the axial components contribute and these will be denoted by w_x' and v_x' for the pressure and vorticity waves respectively. w_x' is related to the pressure amplitude by equation 9, and the axial component of the vorticity wave amplitude is $v_x' = v' \cos\beta$ where β is given by equation 5. It is convenient to work with the velocity perturbations non-dimensionalised with respect to the local speed of sound, a. Recalling that the axial velocity perturbation associated with the pressure wave is given by $\frac{w_x'}{a} = A_x \frac{p'}{\gamma p}$

the total axial velocity perturbation is

$$\frac{U'}{U} = \frac{1}{M_x}\left(A_x \frac{p'}{\gamma p} + \frac{v'}{a}\cos\beta\right)$$

where M_x is the Mach number of the axial mean velocity. The continuity equation is therefore written

$$\frac{p_1'}{\gamma p_1}\left(1 + \frac{A_{x1}}{M_{x1}}\right) - \frac{s_1'}{c_p} + \frac{v_1'}{a_1}\frac{\cos\beta_1}{M_{x1}} = \frac{p_2'}{\gamma p_2}\left(1 + \frac{A_{x2}}{M_{x2}}\right) - \frac{s_2'}{c_p} + \frac{v_2'}{a_2}\frac{\cos\beta_2}{M_{x2}} \qquad (9)$$

On each side $\frac{p'}{\gamma p}\left(1 + \frac{A_x}{M_x}\right)$ can be expanded to

$$\frac{p_+'}{\gamma p}\left(1 + \frac{A_x}{M_x}\right)_+ + \frac{p_-'}{\gamma p}\left(1 + \frac{A_x}{M_x}\right)_-$$

where subscripts + and − refer to the downstream and upstream going waves respectively.

(b) Energy Continuity Equation

With the assumption of short blades this equation amounts to equating the perturbation in stagnation temperature just upstream and downstream of the blade passages. The steady relation across either a rotor or stator row is

$$T_1\left(1+\frac{\gamma-1}{2}M_1^2\right) = T_2\left(1+\frac{\gamma-1}{2}M_2^2\right)$$

where M_1 and M_2 refer to the Mach number upstream and downstream of the blade row in a frame of reference fixed with respect to the blades. For the sake of brevity $1+\frac{\gamma-1}{2}M^2$ is denoted by $\mathcal{M}$.

After allowing perturbations in the entropy, pressure and velocity, in a manner similar to the mass continuity equation, one obtains

$$\mathcal{M}_2\left[(\gamma-1)\frac{p_1'}{\gamma p_1} + \frac{s_1'}{c_p} + (\gamma-1)M_1\frac{W_1'}{a_1}\right] = \mathcal{M}_1\left[(\gamma-1)\frac{p_2'}{\gamma p_2} + \frac{s_2'}{c_p} + (\gamma-1)M_2\frac{W_2'}{a_2}\right]$$

W' is the total velocity perturbation in the direction of the mean relative flow, which again consists, in general, of two parts, one due to the pressure wave, the other the vorticity wave. The perturbation in the direction of the mean flow relative to the blade row can therefore be written as

$$\frac{W'}{a} = \frac{p'}{\gamma p}\left(A_x\cos\theta + A_y\sin\theta\right) + \frac{v'}{a}\cos\psi$$

where θ is the angle between the axial and the mean flow direction, and $\psi = \theta - \beta$ is the angle between the direction of the vorticity waves, β, and the direction of mean flow. Introducing this into the energy equation gives

$$\mathcal{M}_2\left\{\frac{p_1'}{\gamma p_1}(\gamma-1)\left[1+M_1\left(A_{x1}\cos\theta_1 + A_{y1}\sin\theta_1\right)\right] + \frac{s_1'}{c_p} + \frac{v_1'}{a_1}(\gamma-1)M_1\cos\psi_1\right\}$$

$$= \mathcal{M}_1\left\{\frac{p_2'}{\gamma p_2}(\gamma-1)\left[1+M_2\left(A_{x2}\cos\theta_2 + A_{y2}\sin\theta_2\right)\right] + \frac{s_2'}{c_p} + \frac{v_2'}{a_2}(\gamma-1)M_2\cos\psi_2\right\}$$

(10)

Again the sum of the upstream and downstream pressure waves is to be understood in equation 10, remembering that A_x and A_y are different for upstream and downstream going waves.

(c) Entropy Equation

The present calculations have assumed isentropic flow, and under these conditions the entropy perturbation, as well as the time mean entropy, is conserved, i.e. $s_1' = s_2'$ (11) In consequence $T_1'/T_1 = T_2'/T_2$ and the temperature variation

forming the entropy wave is a fixed fraction of the mean temperature. The assumption of isentropy is convenient but not essential. An approach for treating the case of choked passage flow with a shock and subsonic outlet has been formulated by Horlock [4], but the maximum outlet flow Mach numbers from turbine blades are unlikely to be very much greater than one and the error introduced by ignoring the irreversibility in shocks is likely to be small.

The assumption of isentropy implies that there are no shocks and this provides an additional convenience. If the flow is chocked the outlet flow is sonic or supersonic and in this case the fourth equation is provided by the condition of constant upstream mass flow. If the flow is unchoked the fourth equation is one of constancy of outlet flow angle, discussed immediately below. Clearly with shock waves present the flow could be choked and still have a subsonic outlet velocity.

(d) Kutta condition (subsonic outlet flow)

When the blade pitch approaches zero in the actuator disc assumption the flow leaves the blade passage in the direction of the trailing edges, provided the outlet flow is subsonic, and this will be referred to as the Kutta condition. It is assumed here that the outlet flow angle remains constant at the blade angle even with perturbations in pressure, velocity and temperature. If θ_2 is the outlet angle, the unsteady condition is simply that $\tan\theta_2$ is equal to the ratio of the net axial and circumferential velocity perturbations i.e.

$$\tan\theta_2 = \frac{w'_{y2} + v'_2 \sin\beta_2}{w'_{x2} + v'_2 \cos\beta_2}$$

The vorticity wave is then related to the pressure waves by

$$\frac{v'_2}{a_2}\left(\sin\beta_2 - \cos\beta_2 \tan\theta_2\right) = \frac{p'_2}{\gamma p_2}\left(A_{x2}\tan\theta_2 - A_{y2}\right) \qquad (12)$$

(e) Constant upstream mass flow (supersonic outlet flow)

The direction of a supersonic outlet flow depends on the back pressure and the Kutta condition must then be relaxed.

The fourt equation then uses the fact that once the flow is choked the corrected mass flow $(\dot{m}\sqrt{c_p T_o}/A p_o)$ is constant upstream of a blade row. The mass flow rate is equal to $\rho U A$ and the specific heat is constant so that for a supersonic outlet flow $\rho_1 U_1 \sqrt{T_{o1}} / p_{o1} = \text{const.}$ For small perturbations this may be expanded to the condition that

$$\frac{T_1'}{T_1}\left(M_1^2-1\right) + \frac{U_1'}{U_1}\left(1+\frac{\gamma-1}{2}M_1^2\right) - \frac{W_1'}{W_1}M_1^2\left(\frac{\gamma+1}{2}\right) = 0$$

Using the relation developed earlier this may be rearranged as

$$\frac{p_1'}{\gamma p_1}\left[\frac{\gamma-1}{2}\left(M_1^2-1\right) + \mathcal{M}_1\frac{A_{x1}}{M_{x1}} - \left(\frac{\gamma+1}{2}\right)M_1\left(A_{x1}\cos\theta_1 + A_{y1}\sin\theta_1\right)\right.$$

$$\left. + \left(\frac{M_1^2-1}{2}\right)\frac{s'}{c_p} + \frac{v_1'}{a_1}\left(\mathcal{M}_1\frac{\cos\beta_1}{M_{x1}} + \left(\frac{\gamma+1}{2}\right)M_1\cos\psi_1\right) = 0 \right. \qquad (13)$$

4. METHOD OF SOLUTION

Equation (9) and (13) provide a description of blade row behaviour from which the response can be calculated. In principle they could be manipulated algebraically to yield explicit expressions for each output in terms of each input, but this is unattractive, particularly when a succession of blade rows are to be treated.

The procedure chosen utilises the complext matrix handling facilities of a computer. The variables* $p_-'/\gamma p$, $p_+'/\gamma p$, s'/c_p, and v'/a are displayed as column vectors $\overline{V}_1$ and $\overline{V}_2$ on the upstream and downstream sides of a blade row. Equation (9) to (13) form the terms of two four-by-four matrices $\overline{B}_1$ and $\overline{B}_2$, containing terms on the upstream and downstream sides respectively, producing $\overline{B}_1\overline{V}_1 = \overline{B}_2\overline{V}_2$. Whether equation (12) or (13) is used depends on the Mach number of the flow leaving the blade row; if the flow is subsonic at outlet one row of $\overline{B}_2$ contains the terms appropriate to the Kutta condition, whilst the corresponding row in $\overline{B}_1$ contain zeros. If the flow is sonic or supersonic then the same row in $\overline{B}_1$ contains the appropriate terms for the constant upstream Mach number whilst $\overline{B}_2$ contains a row of zeros. The rows of zero constitute

* p_-' and p_+' are the amplitudes of the upstream and downstream propagating pressure waves respectively.

a singularity in the matrices and restrict the way in which they can be handled; at some point a matrix must be inverted and it is important that it should not then be singular.

(a) A single blade row

The matrix form of the equations is $\overline{B}_1 \overline{V}_1 = \overline{B}_2 \overline{V}_2$ where $\overline{V}_1$ and $\overline{V}_2$ are vectors of the variables on the upstream and downstream sides. The solution requires the output variables in terms of the four inputs. It is evident that the vector for the upstream side, $\overline{V}_1$, contains three inputs, $p'_+/\gamma p$, s'/c_p, and v'/a, whilst the upstream going pressure wave, $p'_2/\gamma p$, is an output. Similarly the downstream vector, $\overline{V}_2$, contains three outputs $p'_+/\gamma p$, s'/c_p and v'/a but the upstream going pressure wave, $p'_-/\gamma p$, is an input. It is very easy to rearrange* terms in $\overline{B}_1$ and $\overline{B}_2$ associated with the upstream going pressure waves and to change the vectors so that all inputs and outputs are collected on the left and right hand sides of the equation

$$\overline{B}_I \overline{V}_I = \overline{B}_o \overline{V}_o$$

where subscripts I and O refer to input and output respectively. These matrices, $\overline{B}_I$ and $\overline{B}_o$ will not normally be singular and may be inverted to give the four outputs in terms of the four inputs,

(b) Several Blade row

Between blade rows phase and amplitude variations must be introduced. The expression for the change in phase and amplitude of the pressure, vorticity and entropy perturbations form the terms of a four by four diagonal matrix denoted here by $\overline{T}$. The vorticity and entropy are assumed to be convected without alteration in amplitude, but merely a shift in phase. The pressure waves, which are

---

*with $p'_-/\gamma p$ occupying the same position in the upstream and downstream vector the rearrangement of matrices $\overline{B}$ is particularly easy. It consists of exchanging those terms in $\overline{B}_1$ and $\overline{B}_2$ multiplying $p'_-/\gamma p$, changing the sign of each term as it is exchanged.

above cut-off will also only have a shift in phase. The relative phase lead of the vorticity and entropy wave just downstream of one blade row relative to the wave just upstream of the next blade row downstream can be written $\delta x \left(\omega/V_x \pm \frac{2\pi}{Y}\frac{V}{U}\right)$ where δx is the axial separation between the blade rows and the + sign corresponds to waves propagating to the right. The phase and amplitude variation of the pressure waves can be obtained directly from the axial wavenumber (Equation 7 and 8), and conditions at the upstream row are related to those downstream by a relation such as $e^{-i k_R \delta x} \; e^{k_I \delta x}$

It is convenient to consider two blade rows in the same manner as the isolated row. Across the upstream row

$$\bar{B}_{U1}\,\bar{V}_{U1} = \bar{B}_{U2}\,\bar{V}_{U2} \tag{14}$$

and across the downstream row

$$\bar{B}_{D1}\,\bar{V}_{D1} = \bar{B}_{D2}\,\bar{V}_{D2} \tag{15}$$

The vector $\bar{V}_{U2}$ just downstream from row 1 can be related to the vector $\bar{V}_{D1}$ just upstream from row 2 by

$$\bar{V}_{U2} = \bar{T}\,\bar{V}_{D1} \tag{16}$$

Introducing equation (16) into (14) gives

$$\bar{B}_{U1}\,\bar{V}_{U1} = \bar{B}_{U2}\,\bar{T}\,\bar{V}_{D1} \tag{17}$$

or $$\bar{V}_{D1} = \left(\bar{B}_{U2}\,\bar{T}\right)^{-1}\bar{B}_{U1}\,\bar{V}_{U1}$$

This in turn can be put into equation (15) to give

$$\bar{B}_{D1}\left(\bar{B}_{U2}\,\bar{T}\right)^{-1}\bar{B}_{U1}\,\bar{V}_{U1} = \bar{B}_{D2}\,\bar{V}_{D2} \tag{18}$$

The resulting square matrix on the left and the matrix on the right are then rearranged, just as before for the isolated blade row, to collect the variables into input and output vectors, $\bar{B}_I\,\bar{V}_I = \bar{B}_o\,\bar{V}_o$,after which $\bar{B}_o$

is inverted to give the output variables in terms of the inputs.

If more than two blade rows are present the matrix multiplication leading to equation (18) is repeated for successive rows until the final blade row has been included when, as before, the matrices are rearranged to give input and output vectors and the final inversion carried out.

The calculation procedure will break down if a blade row other than the last is choked. This is because the matrix on the downstream side, $\bar{B}_{U2}$, in equation (17), must be inverted, and if the row is choked $\bar{B}_{U2}$ contains a row of zeros. The calculation of this case requires a different procedure in which the matrices across each blade row are first rearranged into input and output form before being combined. For the sake of brevity this is not described in detail.

5. ACOUSTIC POWER CONSIDERATIONS

The noise nuisance from a jet engine is more likely to be related to the acoustic power propagating downstream from the turbine than to the amplitude of the pressure waves themselves. No attempt will be made to account for reflections from variations in the geometry downstream of the turbine and in the engine propulsion nozzle, or to assess the effect of the jet shear layer on the acoustic power.

Acoustic power from cascades has been examined by Whitehead[5] using the approach of Bretherton and Garret[6]. According to this the acoustic power crossing a section is given by

$$W = \int_A n_j c_j \frac{\bar{p}'^2}{\rho a^2} \frac{\omega}{\omega'} dA$$

provided the wave system is locally above cut-off.

$\bar{p}'$ is the root mean square amplitude of the pressure fluctuation and $n_j c_j$ is the component of the pressure wave group velocity in a direction normal to the area, A , over which the integration is taking place. The group velocity contains one term due to convection by the flow and another due to the propagation; in the present notation (where the area is normal to the axial direction) $n_j c_j = U + a \cos\alpha$

ω' is the Doppler-shifted frequency observed in the frame of reference moving with the flow

$$\omega' = \omega/(1 + M\cos(\theta - \alpha))$$

where M is the resultant Mach number of the mean flow inclined at α to the axial. If the annulus area just downstream of the turbine is A, the acoustic power propagated downstream due to either the left or right wave is given by

$$W = (M\cos\theta + \cos\alpha)(1 + M\cos(\theta - \alpha))\, A a \overline{p'^2}/\gamma p$$

The entropy fluctuation out of the combustor can be described by the standard deviation of the temperature over the mean temperature, σ_T/T (where $\sigma_T^2 = \overline{(T - \bar{T})^2}$). If the downstream pressure perturbation is taken to be related to the temperature fluctuation by $(p'/\gamma p)^2 = f_{TP}\,(\sigma_T/T)^2$, the acoustic power can be written as

$$W = (M\cos\theta + \cos\alpha)(1 + M\cos(\theta - \alpha))\, f_{TP} \left(\frac{\sigma_T}{\bar{T}}\right)^2 \gamma a p A \qquad (19)$$

Although equation (19) appears to be independent of the frequency both α and f_{TP} are in fact functions of frequency. The calculation of power from a broad band entropy input requires an integration with respect to frequency of equation (19) in which σ_T^2 is replaced by the spectral density.

6. THE RESULTS OF CALCULATIONS PERFORMED

The calculations produce a very large number of results and it would be impractical to illustrate more than a few. For the left and right hand waves the amplitude and phase of the upstream and downstream going pressure wave and the vorticity wave are calculated for an input consisting of entropy, vorticity and upstream and downstream pressure waves. The results shown here will consist of pressure waves due to entropy wave inputs and the pressure waves reflected or transmitted for an incident pressure wave. The blade row response is frequency dependent and it is convenient to take fY/a as the independent variable where f is the frequency in Hz, Y is the wavelength along the cascade and a is the speed of sound in the flow into the blade row, into the first blade row if there is more than one. When more than one blade row is

being considered the axial spacing δx must be specified, but it is physically more relevant to use $\delta x/Y$.
In the first part of this section some results obtained from isolated blade rows are examined and in the second part a few results from combinations of blade rows are given.

(a) Isolated blade row

Figure 2 shows the amplitudes of the pressure perturbations on the upstream and downstream side of a blade row when an entropy wave of unit amplitude impinges. The blade row typifies a nozzle guide vane (NGV) with a low Mach number, axial inlet flow and a high subsonic, highly skewed outlet flow, $M_2 = 0.95$, $\theta_2 = 70.39^\circ$. For the sake of definiteness the height of the blade is assumed constant. The peak in the upstream and downstream pressures occurs at the point of cut-off for that region and that wave. Upstream of the blade row the flow is axial and the cut-off value of fY/a is identical for the left and right hand wave systems. The cut-off peak on the upstream side produces a trough on the downstream side. The downstream peak in the left hand wave barely produces any effect upstream, however, and this can be explained by the high outlet Mach number reducing the influence of downstream conditions. The calculations very close to the peaks and troughs associated with cut-off become relatively inaccurate and it must be inferred that the analysis predicts infinite amplitude at the peak, and zero in the trough, but this is, in any case, a consideration of purely academic interest. The results for the supersonic outlet counterpart of the nozzle described above are shown in Figure 3. The inlet conditions and outlet flow angle are the same and only the outlet Mach number is increased to 1.05. The variation in amplitude of the pressure waves due to an entropy wave input is very similar to that for the subsonic blade row, but the magnitudes are slightly greater. Because the downstream conditions can have no effect upstream when the outflow is supersonic, it is not surprising to find no evidence upstream of the peak around the downstream cut-off of the left hand wave.

The similarity of the pressure wave output for a subsonic and a supersonic outlet is striking, but the similarity of the shed vorticity, Figure 4, is even more remarkable. The

amplitude is slightly greater for the supersonic case but beside this the only difference is in the "corner" for the left-hand downstream wave close to the cut-off. The "corner" is abrupt for the subsonic case, where a Kutta condition is applied, but gradual for the supersonic case when the Kutta condition is replaced by the requirement of constant upstream mass flow. The discontinuity for the subsonic case is very likely to be connected with the coincidence in the direction of velocity perturbations arising from the vorticity and pressure waves at the cut-off point. This is because the Kutta condition seeks to add these perturbations in such a way as to make the resulting perturbation parallel to the trailing edge, which, in general, is impossible when the direction of the perturbations is the same.

The results of Figure 5 are an attempt to compare the downstream pressure wave amplitude due to entropy wave inputs for a range of blade deflections and accelerations. In each case the blading is assumed to be of constant height and it is this which determines the inter-relation of Mach number and direction. Compared to the results shown in Figures 2 and 3 it would seem that the amplitudes are decreased if the inlet Mach number is raised or the outlet Mach number reduced. A non-axial flow at inlet does not appear to have a significant affect other than to alter the behaviour near to the cut-off condition on the upstream side. In summary it appears that the overiding effect in determining the amplitude of pressure waves produced by vorticity interactions with a blade row is acceleration of the flow through the row.

Figure 6 shows the response of the subsonic blade row (used in Figure 2 for entropy wave input) when exposed to a downstream going pressure wave. The variation in amplitude of the transmitted, downstream going wave with respect to fY/a is very similar to the variation observed with an entropy wave input. The reflected wave, however, shows quite a different character with a trough at the upstream cut-off frequency. The vorticity wave shows the discontinuous shape for the left hand wave noticed with the entropy wave into an unchoked blade row.

Attention was drawn to the significance of the flow acceleration in producing pressure waves from entropy. In test cases where there was no overall flow acceleration through the blade row the entropy was found to produce no pressure or vorticity waves. This was even true of impulse type blades with large flow deflection ($\theta_1 = -\theta_2$) but equal inlet and outlet Mach number. Pressure or vorticity waves incident on non-accelerating blade rows do, however, produce new pressure and vorticity waves. Figure 7 compares the transmitted and reflected pressure waves obtained using the present method with results calculated by Kaji and Okazaki[7] and Smith[8]. The results shown are the transmitted and reflected pressure wave amplitudes for an upstream pressure wave incident on an uncambered cascade staggered at 60°. Both the calculations by Kaji and Okazaki and by Smith take into account the finite chord length and pitch in satisfying the boundary conditions on the blades. Whilst the agreement between the present actuator disc method and these other methods is remarkable, it is not altogether surprising in view of the agreement Kaji and Okazaki found between their full method and their semi-actuator-disc method. Although their semi actuator disc method included the blade chord, the effect of the chord was shown to be relatively small. At this point it is perhaps worth mentioning that although the present method had to be made to cope with the vorticity shed by upstream blades with fluctuating lift it is, in fact, more general. It can be used, like those of Kaji and Okazki and Smith, to obtain the pressure wave amplitudes due to vorticity inputs arising from the wakes of upstream bodies or ingested inflow distortion.

The special case of no deflection or acceleration was considered above. In another special case the flow remains axial but is accelerated by a variation in the blade height (normal to x and y). When fY/a tends to infinity the wave fronts become parallel to the y direction and the model then represents plane waves through a straight, one-dimensional nozzle. The response of a very short one-dimensional nozzle due to small amplitude entropy perturbation can be analysed very easily and the pressure amplitude calculated by hand*. For inlet and outlet Mach numbers of 0.2 and 0.95 respectively the downstream going pressure wave amplitude due to a unit amplitude entropy wave

---

*The expression is $\frac{p_2'}{\delta p_2} = \frac{1}{2}\frac{s'}{c_p}\frac{M_2^2 - M_1^2}{1+M_2^2}\frac{M_2}{M_2(1+\frac{\gamma-1}{2}M_1^2)+M_1(1+\frac{\gamma-1}{2}M_2^2)}$

input is 0.177. Using the blade row program described above with axial flows, the same Mach numbers and taking $\delta Y/a = 100$ the downstream pressure wave amplitude was found to be exactly equal to 0.177.

(b) Several blade rows

The range of possible test cases rises alarmingly with the introduction of several blade rows and only a very few examples are shown here.

Figure 8 shows the downstream pressure wave amplitude due to entropy waves into a single turbine stage consisting of a row of nozzles followed by a rotor. The height of the blades remains constant and the nozzle blades are those used for Figure 2 with an axial inlet Mach number of 0.2 and an outlet Mach number of 0.95. The results of Figure 8 are for three different axial spacings and at the largest there is clear evidence of axial resonance effects. This axial spacing, $\delta x/y = 0.32$ is too large for a typical turbine stage, but in multistage turbines with up to 10 blade rows the total axial length does become large and such effects have been noticed.

The turbine loading for the turbine stage represented by Figure 8 was fairly high and so Figure 9 compares the downstream pressure amplitudes for two stages of different rotor loading. The higher loading is the same as that of Figure 8 and for both cases the axial separation is equal to the middle value used for Figure 8. The very strong dependence of pressure amplitude on turbine loading is evident and this is consistent with what was found for isolated blade rows where the pressure amplitude rose sharply with the flow acceleration in the blade row.

Compared with the results for the nozzles alone, Figure 2, two features deserve pointing out. First, the levels are considerably higher for the stages compared with the nozzles. Second, the higher downstream pressure amplitudes were found with the left hand waves for the nozzle whereas the situation is reversed for the stage, with the right hand waves generally having higher amplitudes.

The downstream spectra of acoustic power shown in Figure 10

are due to entropy waves into the nozzle guide vanes alone and the more heavily loaded stage of Figure 9. The power is clearly much greater for the stage. For the right hand waves from the full stage and the left hand waves of the nozzles it is possible to see a very common trend in plots of power against frequency. The power rises quite rapidly as fY/a is reduced until, just before the point of cut-off, there is a precipitous fall. Although the pressure amplitude at cut-off appears to be infinite the cut-off condition requires that no power is actually transmitted.

Figure 11 shows the final example to be given here and gives the spectra of non-dimensional acoustic power due to an entropy wave into turbines with different numbers of stages. The stages all have 50% reaction and "repeat", that is to say the flow Mach numbers and directions are the same for each stage. The fall in temperature across each stage, however, leads to a drop in the acoustic velocity. For this reason the cut-off value of fY/a at outlet falls with the number of stages. The axial separation ($\delta x/Y$ = 0.032 for the first stage) has also been varied to allow for the fall in a. The peak spectral density of acoustic power increases with the number of stages, with a shift towards the lower values of fY/a. The integral of the power with respect to frequency is, however, virtually constant for two or more stages. The power curves show the tendency to rise with fall in fY/a followed by a precipitous drop at the point of cut-off.

If in Figure 11 an attempt is made to average the 2,3 or 4 stage results in the range of fY/a up to 5, a value around 0.035 might be obtained for the sum of the left and right hand waves. Taking realistic values for a, p, σ_T/T and A (say 500 m/s, 1.5 10^5 N/m^2, 0.02 and 0.5 m^2 respectively) and assuming a constant ("white") spectrum of $\sigma_T(\omega)$ up to the top frequency, would give an acoustic power of 500 watts or 148dB re 10^{12} watts. This represents a very large amount of acoustic energy, quite comparable to that obtained from even large aircraft engines at reduced thrust.

CONCLUSIONS

1. The small fluctuations in the temperature of the gas entering a turbine are able to produce large amounts of acoustic power, at least comparable to the power radiated by large aero-engines at reduced thrust.

2. The acoustic power from two identical stages is greater than for one stage. Further identical stages do not increase the overall power although the spectrum shifts to lower frequencies with a higher peak.

The power also increases with stage loading and is markedly higher for a stage compared with a nozzle guide vane row alone.

3. The pressure amplitude produced by an entropy fluctuation into a blade row rises to peak at the cut-off condition. Using the linearised analysis described here the amplitude of the peak is infinite.

4. The pressure wave amplitudes produced by an entropy wave interacting with an isolated blade row increase with the degree of flow acceleration through the row and are zero for blades producing no overall acceleration. The overall behaviour is not very different for blades with either subsonic or supersonic outlet velocities.

5. In the case of an uncambered blade row with no flow deflection or acceleration, predictions using the present actuator disc method of the reflection and transmission of incident pressure waves agree very well with more elaborate analyses taking account of finite blade pitch and chord.

6. The analysis can only be rigorously justified for low frequencies. The agreement with Kaji and Okazaki and Smith suggests, however, that it remains accurate up to at least moderate reduced frequencies. The upper limit will reduce as flow Mach number rises.

NOMENCLATURE

a	Local speed of sound
A	Cross-sectional area
A_x A_y	$w'_x/a = A_x\, p'/\gamma p$ $\quad w'_y/a = A_y\, p'/\gamma p$
$\bar{B}_1$ $\bar{B}_2$	Matrix from left and right sides of equations 9-13
c_p	Specific heat at constant pressure
f	Frequency, Hz
k	Axial Wavenumbers of pressure wave
M	Mach number of resultant mean velocity,
m	$1 + \frac{\gamma-1}{2} M^2$
p	Static pressure
s	Entropy
T	Static temperature
U V	Axial and Circumferential mean flow velocities
v'	Velocity perturbation from vorticity wave
w'	Velocity perturbation from pressure wave
$\bar{V}$	Vector $[k'/\gamma p,\ p'_t/\gamma p,\ s'/c_p,\ v'/a]$
W	Resultant mean flow velocity
x y	Distance in axial and circumferential direction (normal and parallel to cascade) respectively
Y	Wavelength in y direction
α	Angle between pressure wave propagation direction and axial
β	Angle between pressure vorticity wave fronts and axial
γ	Ratio of specific heats
δx	Axial spacing between blade rows
θ	Angle between mean flow direction and axial
ρ	Density
σ_T	Standard deviation in temperature
ϕ	Phase angle
ψ	$(\theta - \beta)$
ω	Radian frequency

Superscript

$'$	Perturbation
$\wedge$	Peak value

Subscript

1 2	upstream and downstream
x y	components in x and y direction
R I	Real and imaginary

$-$ $+$ Upstream and downstream going (refers to pressure waves)

u d Upstream and downstream blade rows

r o Input and output

o Stagnation proterties

REFERENCES.

1. R.R. Dils. "Dynamic Gas Temperature Measurements in a Gas Turbine Transition Duct Exit"
A.S.M.E. Paper 73-GT-7

2. S.M. Candel "Analytical Studies of some acoustic problems of jet engines"
California Institute of Technology
Ph.D. Thesis 1972.

3. J.M. Tyler and T.G. Sofrin "Axial Flow Compressor Noise Studies"
S.A.E. Trans., Vol. 73

4. J.H. Horlock Private communication

5. D.S. Whitehead "Vibration and Sound Generation in a cascade of flat plates in subsonic flow"
A.R.C. Report and Memorandum 3685, 1972.

6. F.P. Bretherton and C.J.R. Garrett. "Wavetrains in inhomogenous moving media".
Proc. Roy. Soc. A302 p 524 (1968)

7. S. Kaji and T. Okazaki "Propagation of sound waves through a blade row. II Analysis based on acceleration potential method".
J. Sound Vib. Vol. 11, p. 355, 1970

8. S.N. Smith "Discrete frequency sound generation in axial flow turbomachines"
A.R.C. Report and Memorandum 33574, 1972

ACKNOWLEDGMENTS

The authors wish to thank Dr. D.S. Whitehead for his help in discussing some aspects of this work, and in particular for his assistance with the method of solution.

The help of Drs. R.R. Dils and E.M. Greitzer of Pratt and Whitney aircraft is greatly appreciated.

APPENDIX

The velocity and pressure perturbations in the pressure waves are linearly related so that the exponential dependence of the w_x and w_y velocity perturbation normal and parallel to the cascade will be the same as that of the pressure. The exponential forms of equation 6 must be substituted in the linearised equations of motion

$$\frac{\partial w_x'}{\partial t} + U\frac{\partial w_x'}{\partial x} + V\frac{\partial w_x'}{\partial y} = -\frac{1}{\rho}\frac{\partial p'}{\partial x}$$

$$\frac{\partial w_y'}{\partial t} + U\frac{\partial w_y'}{\partial y} + V\frac{\partial w_y'}{\partial y} = -\frac{1}{\rho}\frac{\partial p'}{\partial y}$$

A1

It follows after some cancellation that

$$\left(-\omega + Uk \pm V\frac{2\pi}{Y}\right) w_x' e^{i\phi_x} = -k\frac{p'}{\rho}$$

$$\left(-\omega + Uk \pm V\frac{2\pi}{Y}\right) w_y' e^{i\phi_y} = \pm\frac{2\pi}{Y}\frac{p'}{\rho}$$

A2

where ϕ_x and ϕ_y are the phase differences between the x and y components of the velocity perturbation and the pressure. If the wave system is above cut-off, k is real and ϕ_x and ϕ_y are zero so that the velocity perturbations are in phase with the pressure. In this case $\frac{w_y'}{w_x'} = -\frac{\pm 2\pi/Y}{k}$ and it is easy to show that this corresponds to the resultant velocity perturbation, w', being normal to the wavefront and of magnitude such that $\frac{w'}{a} = \frac{p'}{\gamma p}$. For convenience the direction of the velocity perturbation relative to the axial is denoted by α, where $\tan\alpha = -(\pm 2\pi/Y)/k$, and it follows that

$$\frac{w_x'}{a} = \frac{p'}{\gamma p}\cos\alpha$$

$$\frac{w_y'}{a} = \frac{p'}{\gamma p}\sin\alpha$$

A3

In the more complicated condition when the waves system is below cut off it is convenient to divide k into the real

and imaginary parts. Thus

$$k_R = -\frac{2\pi/Y}{1-M_x^2} M_x \left(\frac{\omega}{a}\frac{Y}{2\pi} \pm M_y\right)$$

and

$$k_I = -\frac{2\pi/Y}{1-M_x^2}\left(\pm\sqrt{(1-M_x^2) - \left(\frac{\omega}{a}\frac{Y}{2\pi} \pm M_y^2\right)}\right) \qquad \text{A4}$$

The term in the left hand side of equation A2 can be rewritten and using equation A4 it can be shown that

$$\left(-\omega + Uk \pm V\,2\pi/Y\right) = -2\pi a/Y\left[\left(\frac{\omega}{a}\frac{Y}{2\pi} \pm M_y\right) - M_x\frac{kY}{2\pi}\right]$$
$$= -a\left[k_R/M_x \pm i k_I M_x\right] \qquad \text{A5}$$

where, as before, the + sign before i refers to the upstream going wave.

Introducing A5 into A2 gives

$$\frac{w_x'}{a} e^{i\phi_x} = \frac{k_R + i k_I}{k_R/M_x \pm i M_x k_I}\frac{p'}{\gamma p}$$

$$\frac{w_y'}{a} e^{i\phi_y} = \frac{\pm 2\pi/Y}{k_R/M_x \pm i M_x k_I}\frac{p'}{\gamma p} \qquad \text{A6}$$

where ρ has been replaced by $\gamma p/a^2$. Equation A6 therefore provides the complex form of the velocity perturbation associated with pressure waves below cut-off. In the computation the real and imaginary components of w_x' and w_y' are used, rather than ϕ_x and ϕ_y. The velocity perturbations are proportional to the pressure amplitude and in the analysis it is convenient to use this. If A_x and A_y are complex terms depending on the axial wave number and Mach number in equation A5, then

$$\frac{w_x'}{a} = A_x\frac{p'}{\gamma p}$$

$$\frac{w_y'}{a} = A_y\frac{p'}{\gamma p} \qquad \text{A7}$$

If the waves are above cut-off A_x and A_y are real and equal to $\cos\alpha$ and $\sin\alpha$ respectively.

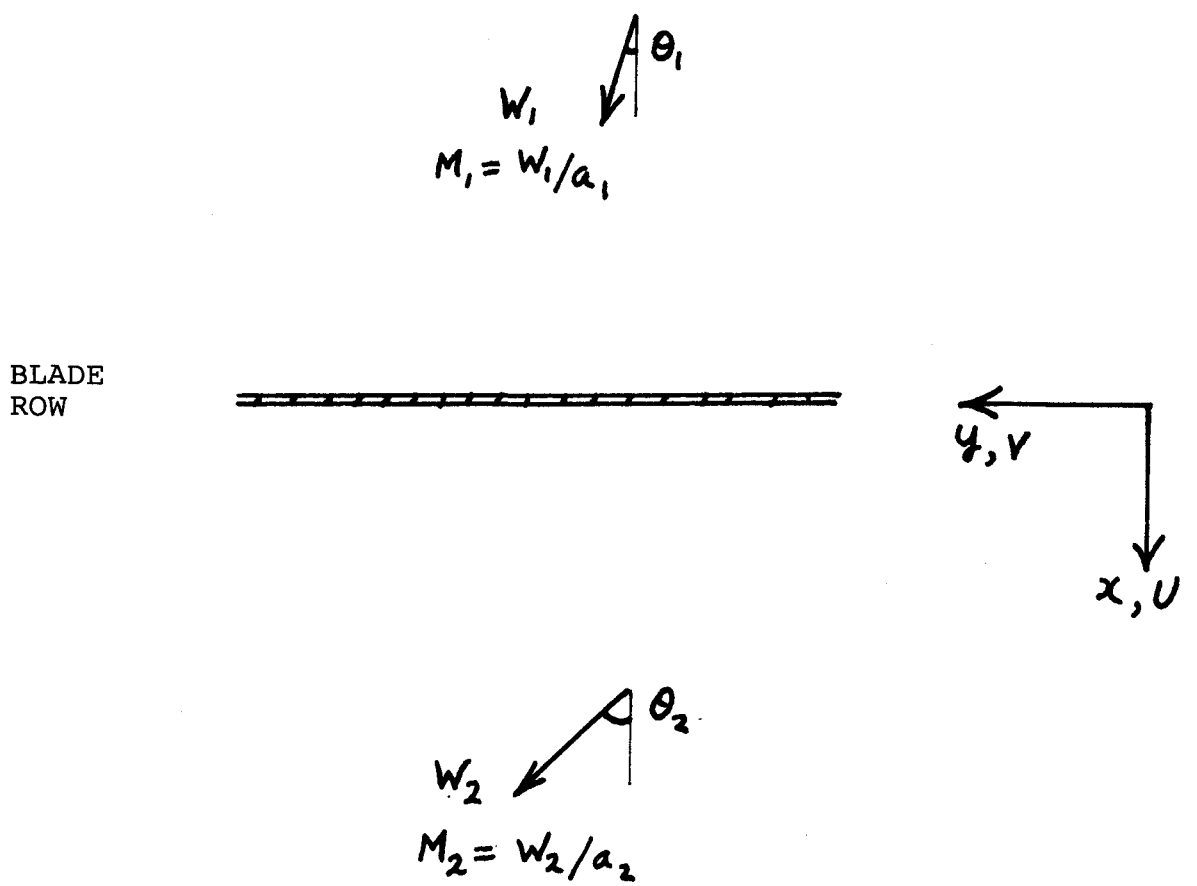

CO-ORDINATE SYSTEM FIG. 1

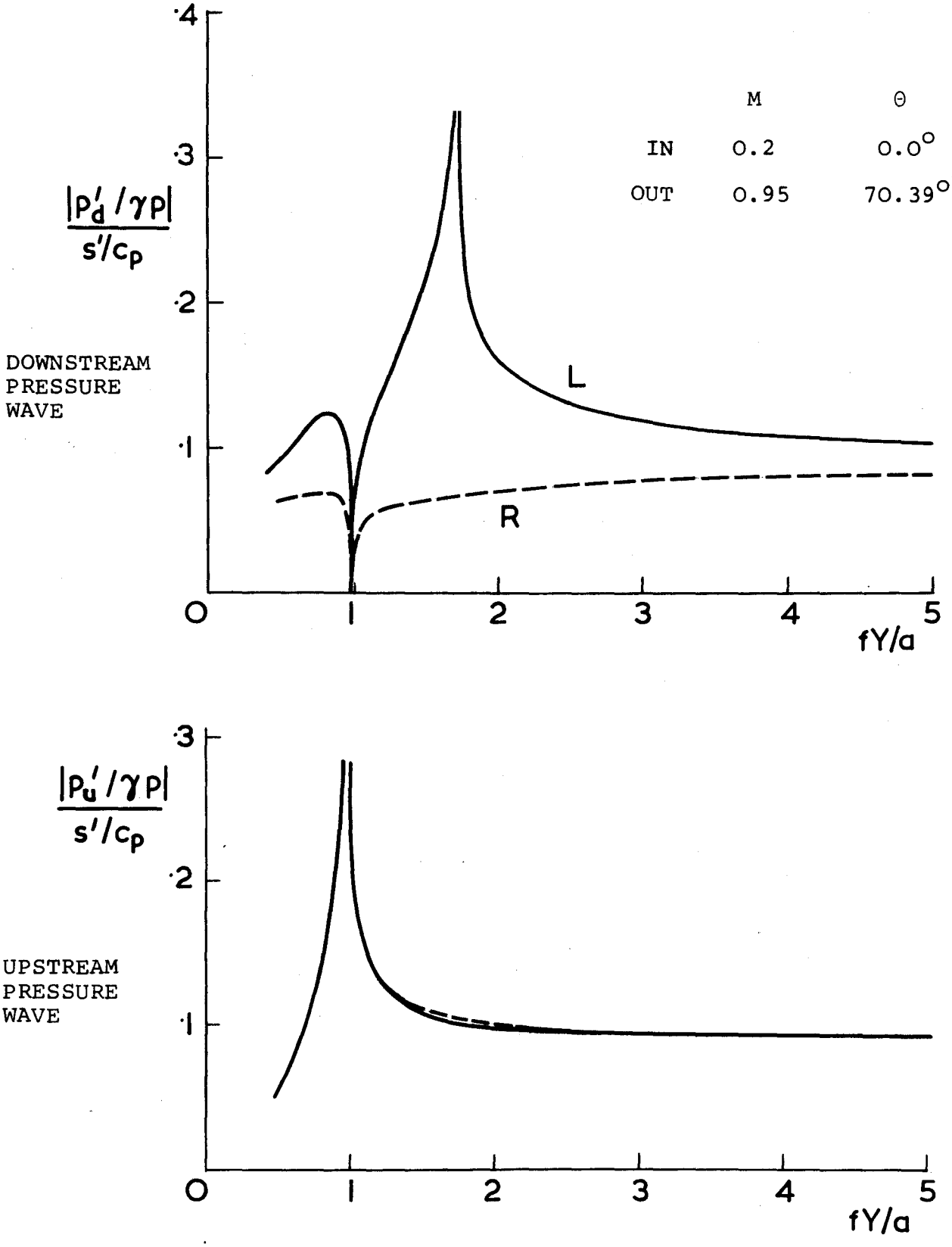

PRESSURE WAVE AMPLITUDES DUE TO ENTROPY WAVE INTO AN ISOLATED ROW OF NGV WITH SUBSONIC OUTLET FLOW

FIG. 2

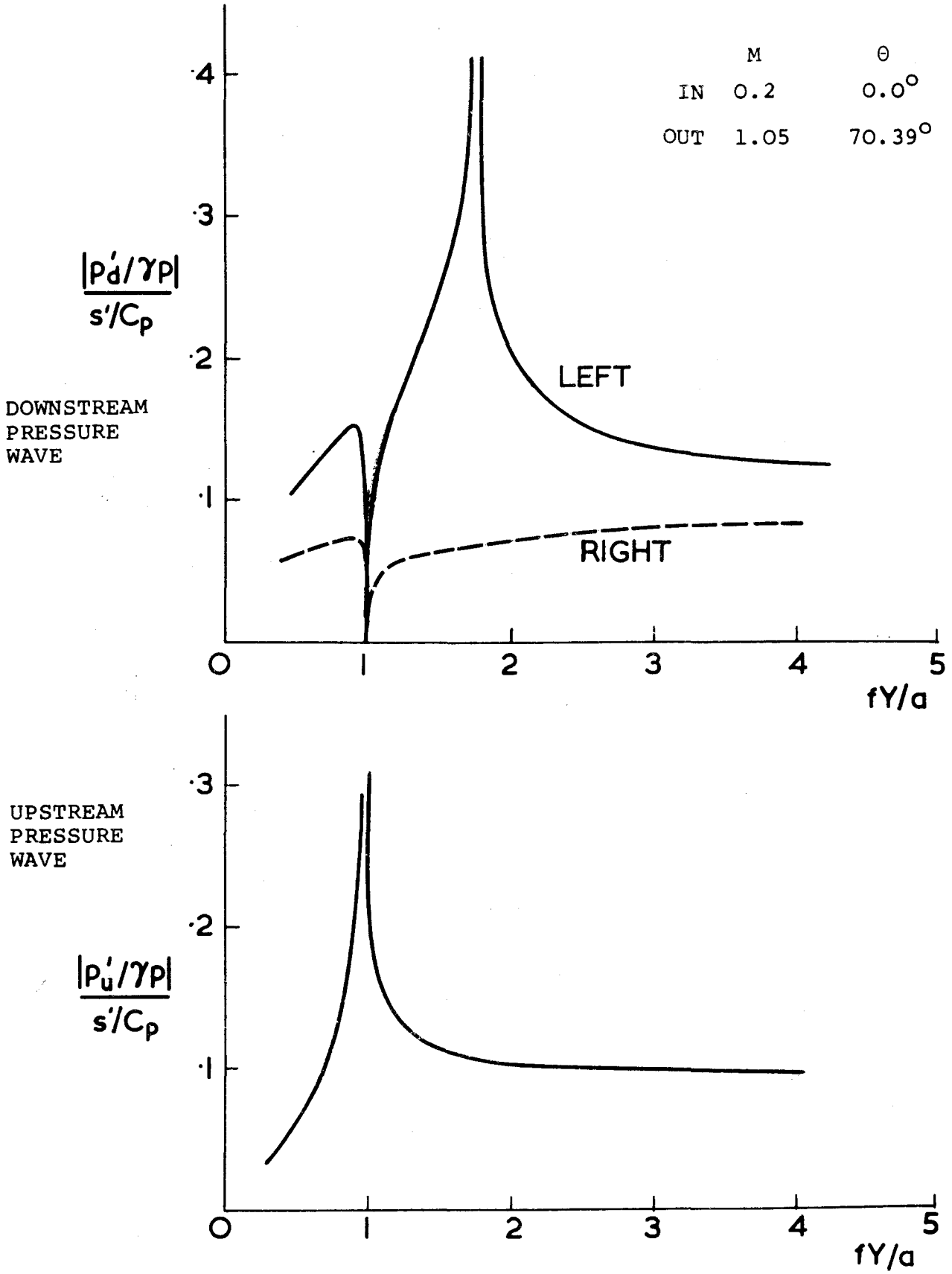

PRESSURE WAVE AMPLITUDES DUE TO ENTROPY WAVE INTO AN ISOLATED ROW OF NGV WITH SUPERSONIC OUTLET FLOW.

FIG. 3

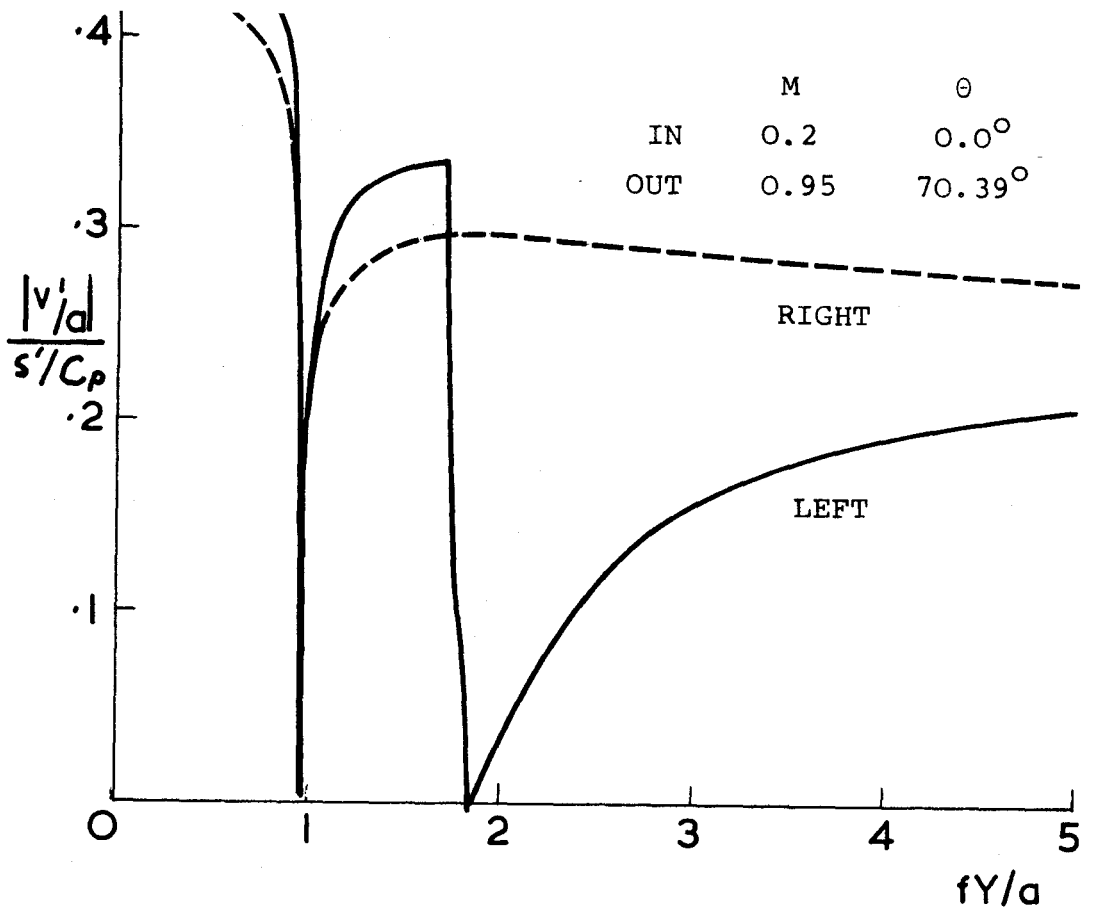

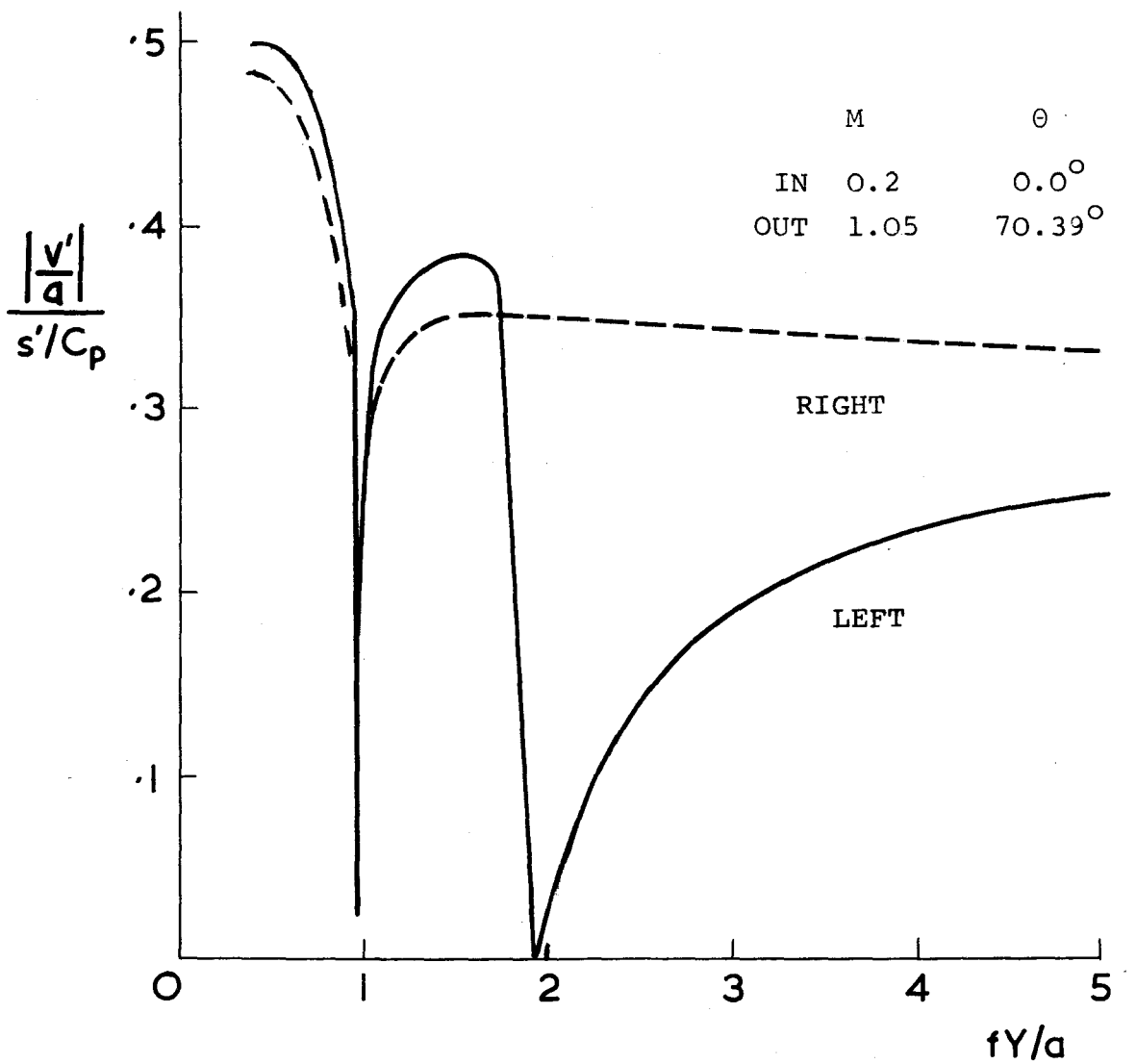

ORTICITY WAVE AMPLITUDES DUE TO ENTROPY WAVE INTO AN ISOLATED ROW OF GV WITH SUBSONIC AND SUPERSONIC OUTLET FLOW. FIG. 4

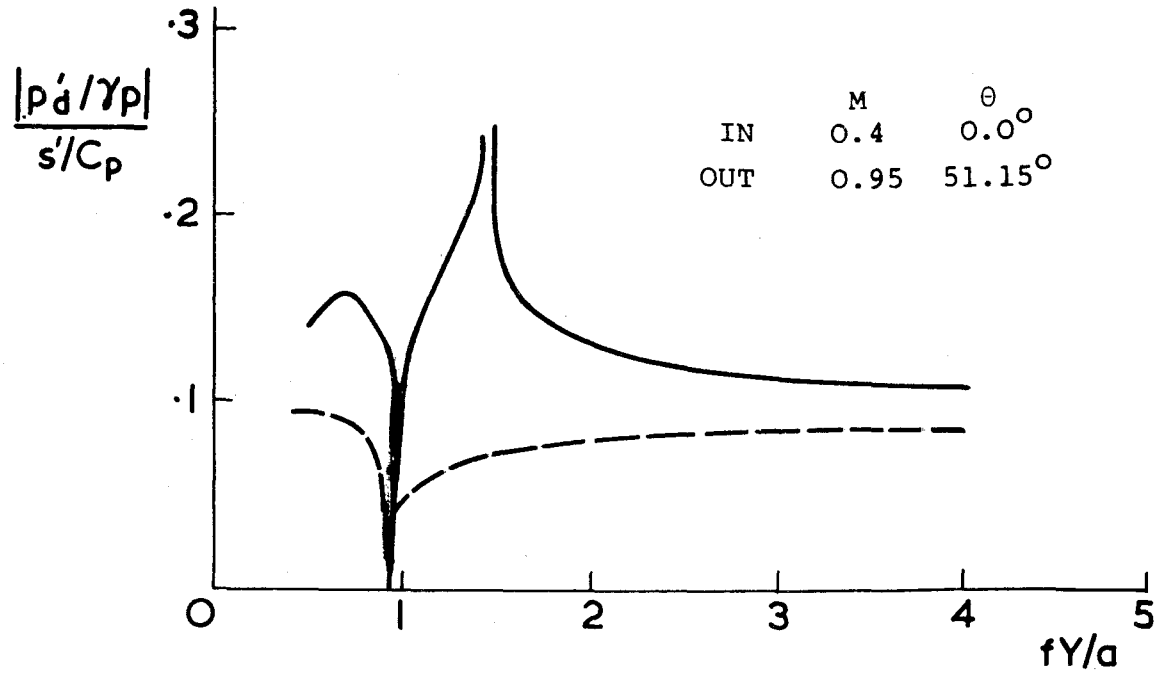

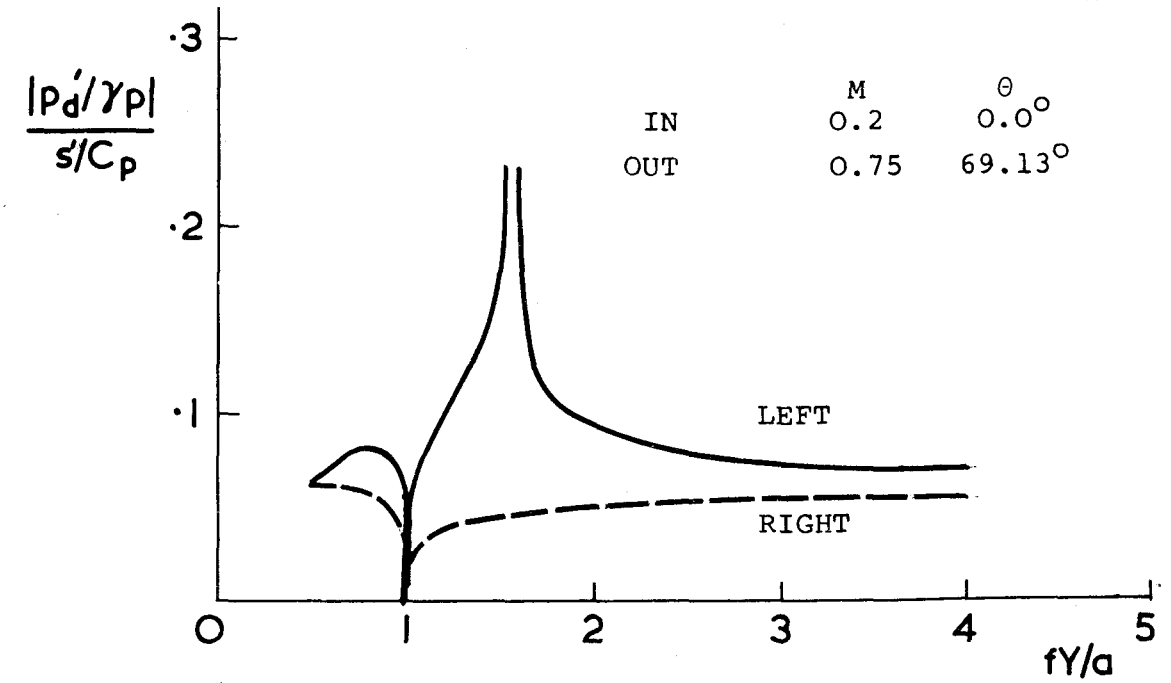

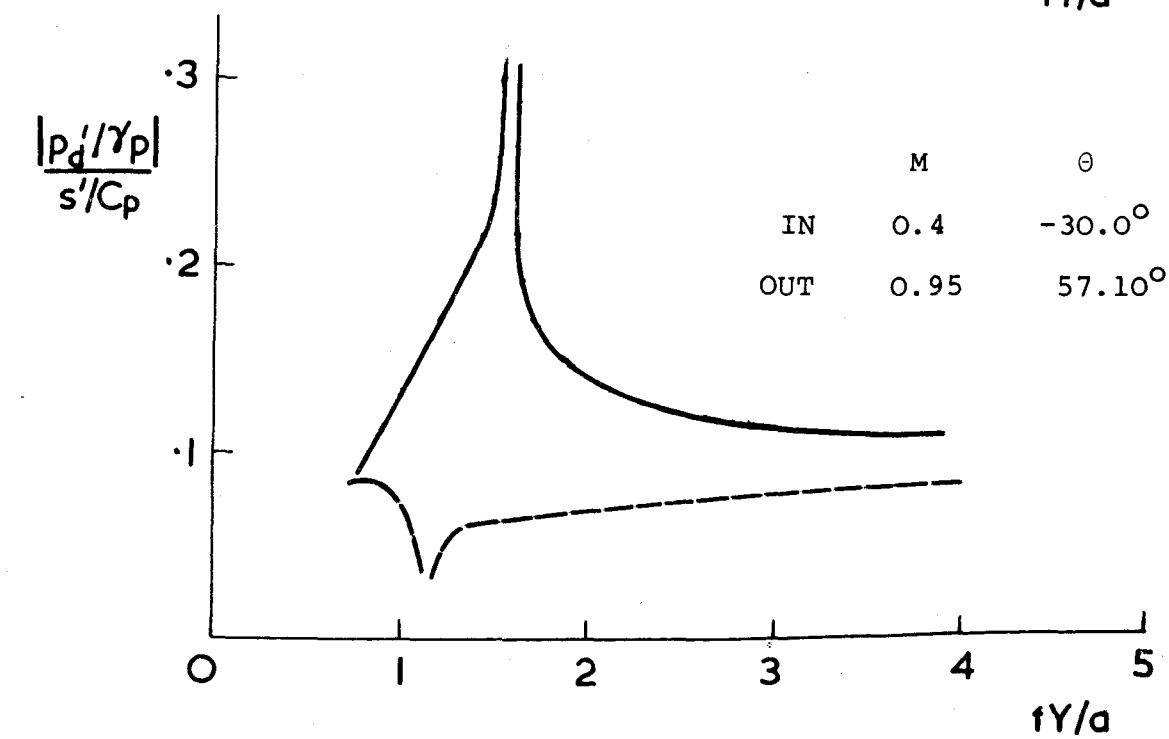

DOWNSTREAM PRESSURE WAVE AMPLITUDES DUE TO ENTROPY WAVE INTO ISOLATED ROW OF NGV WITH DIFFERING SUBSONIC FLOWS.

FIG. 5

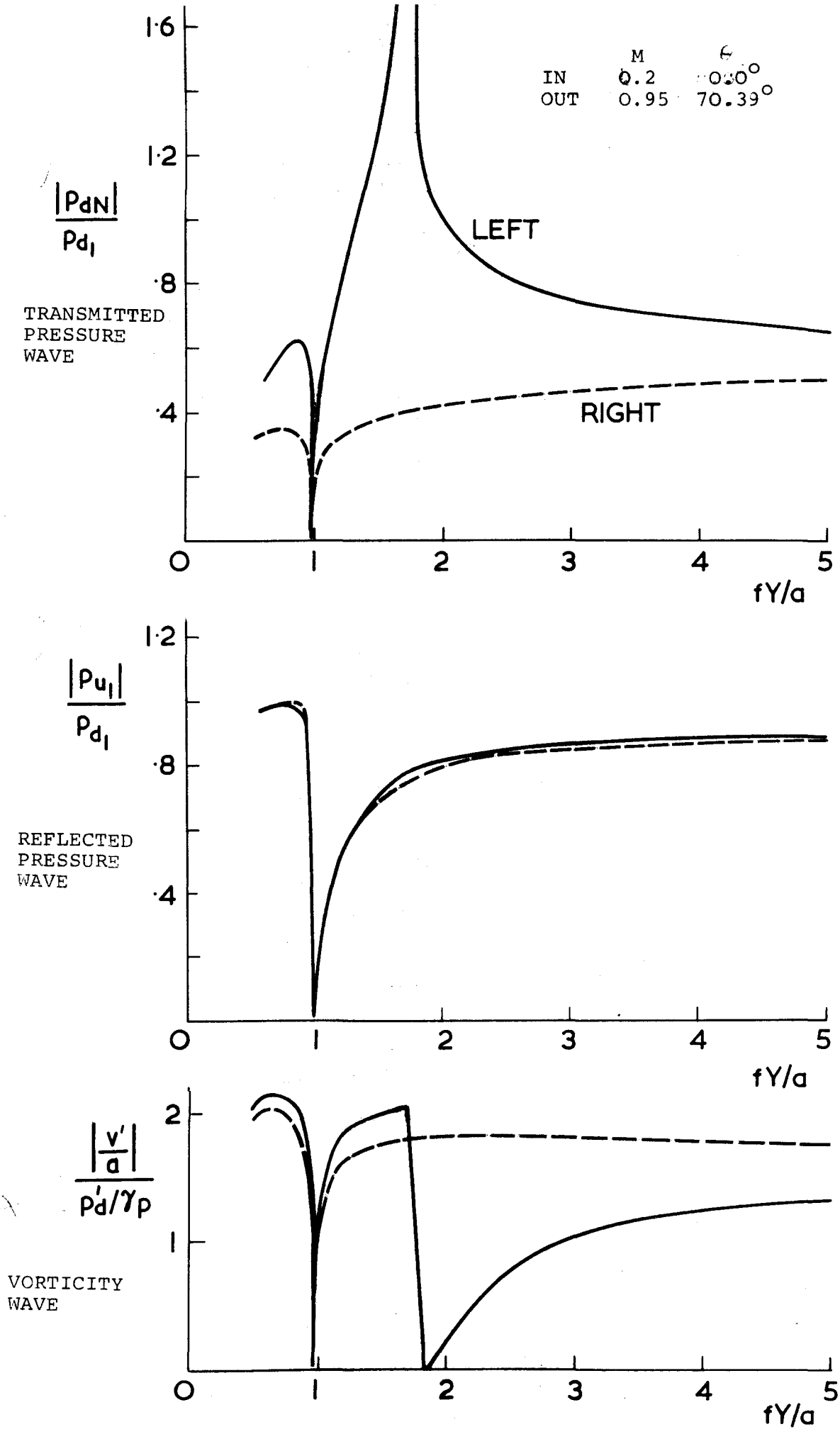

TRANSMITTED AND REFLECTED PRESSURE WAVE AND VORTICITY WAVE AMPLITUDES FOR DOWNSTREAM PRESSURE WAVE INPUT FIG. 6

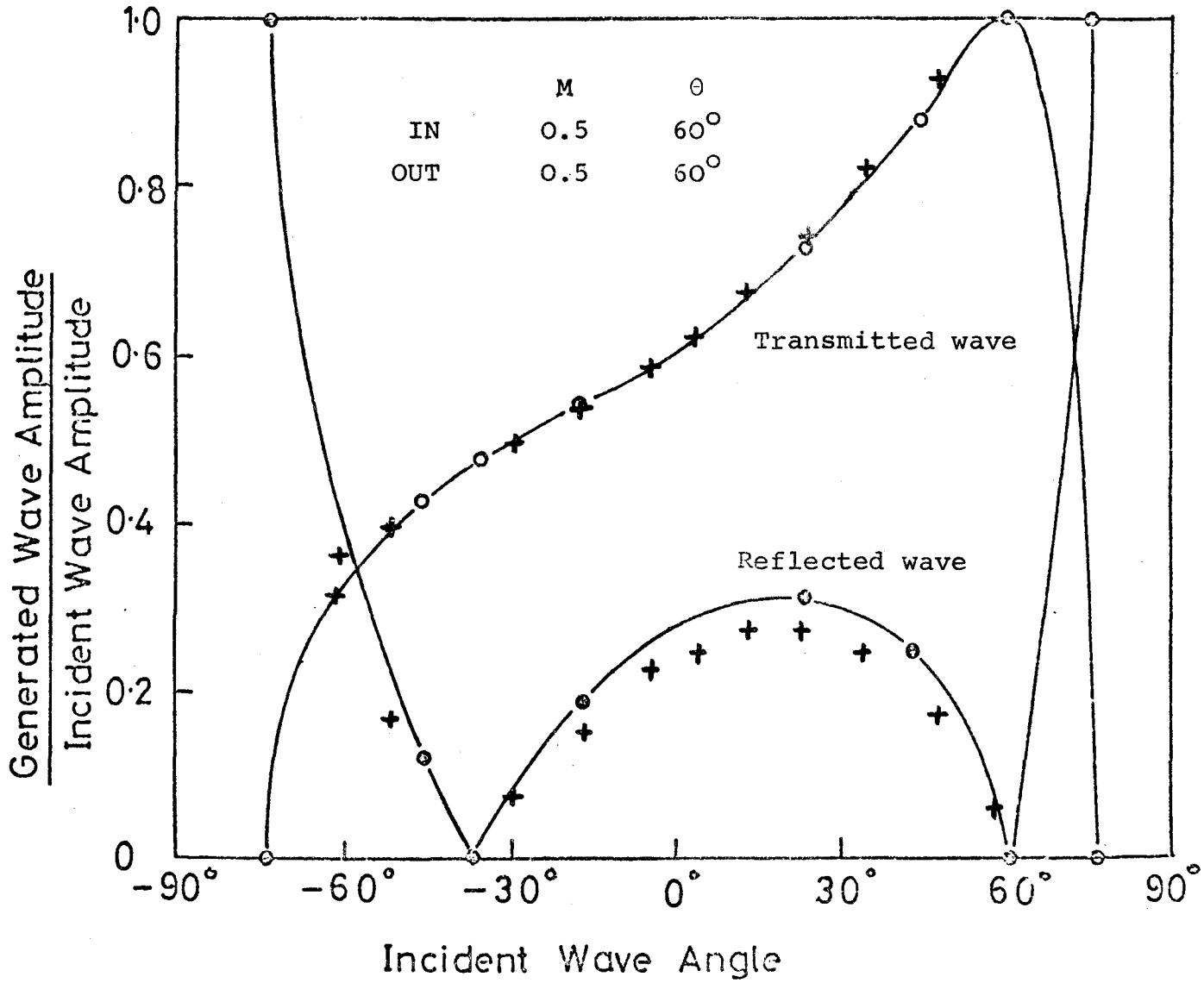

——— Results of Kaji and Okazaki (Ref. 7) } Space chord ratio = 1

o Results of Smith (Ref. 8) } Reduced frequency, $\frac{\omega c}{U} = \frac{\pi}{2}$

\+ Results of present calculation

COMPARISON OF CALCULATIONS USING PRESENT METHOD WITH RESULTS OF OTHER METHODS FOR UPSTREAM GOING PRESSURE WAVE INCIDENT ON UNCAMBERED BLADE ROW.

FIG. 7

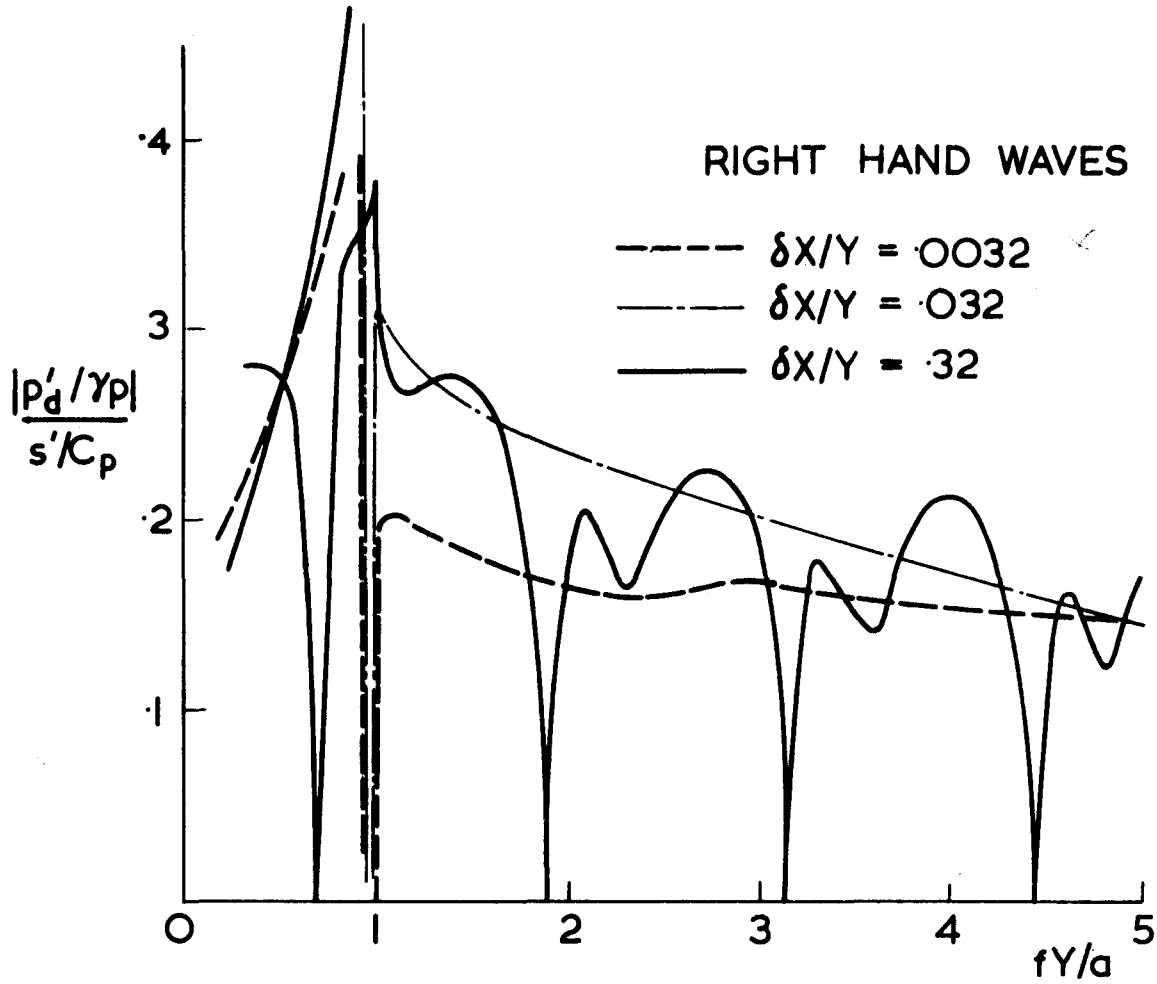

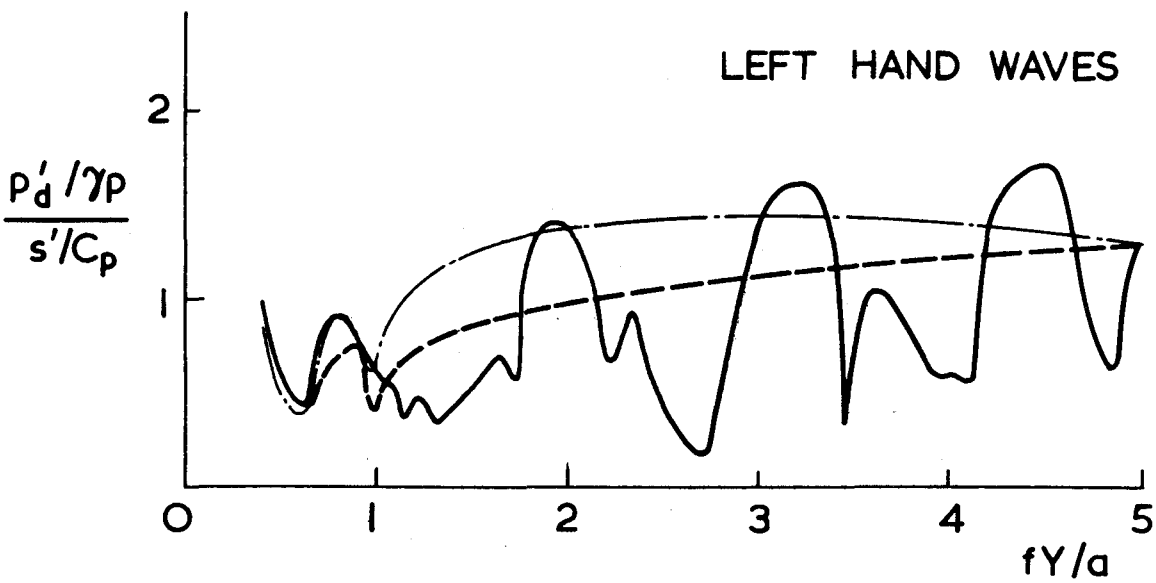

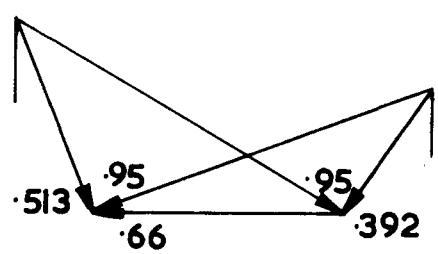

DOWNSTREAM PRESSURE WAVE AMPLITUDES DUE TO ENTROPY WAVE INTO ISOLATED STAGE WITH DIFFERING AXIAL SPACING BETWEEN THE NGV AND ROTOR BLADES FIG. 8

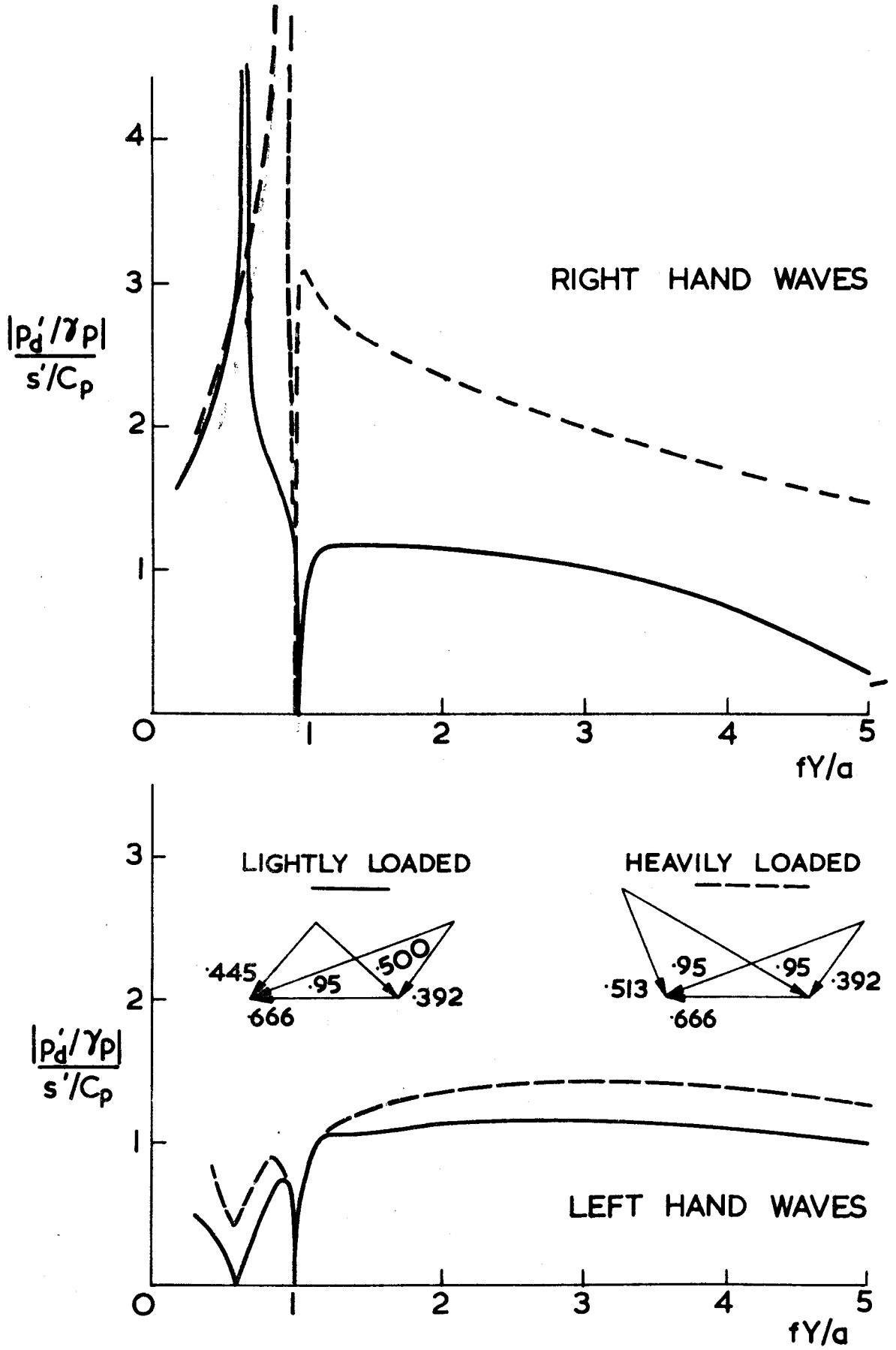

DOWNSTREAM PRESSURE WAVE AMPLITUDE DUE TO ENTROPY WAVES INTO TWO STAGES WITH DIFFERING ROTOR LOADING ($\delta x/Y = 0.032$) Fig. 9

	M	Θ
NGV	(0.2	0.0°
	(0.95	70.39°
ROTOR	(0.39	35.6°
	(0.95	-59.6°

$\delta x/Y = 0.032$

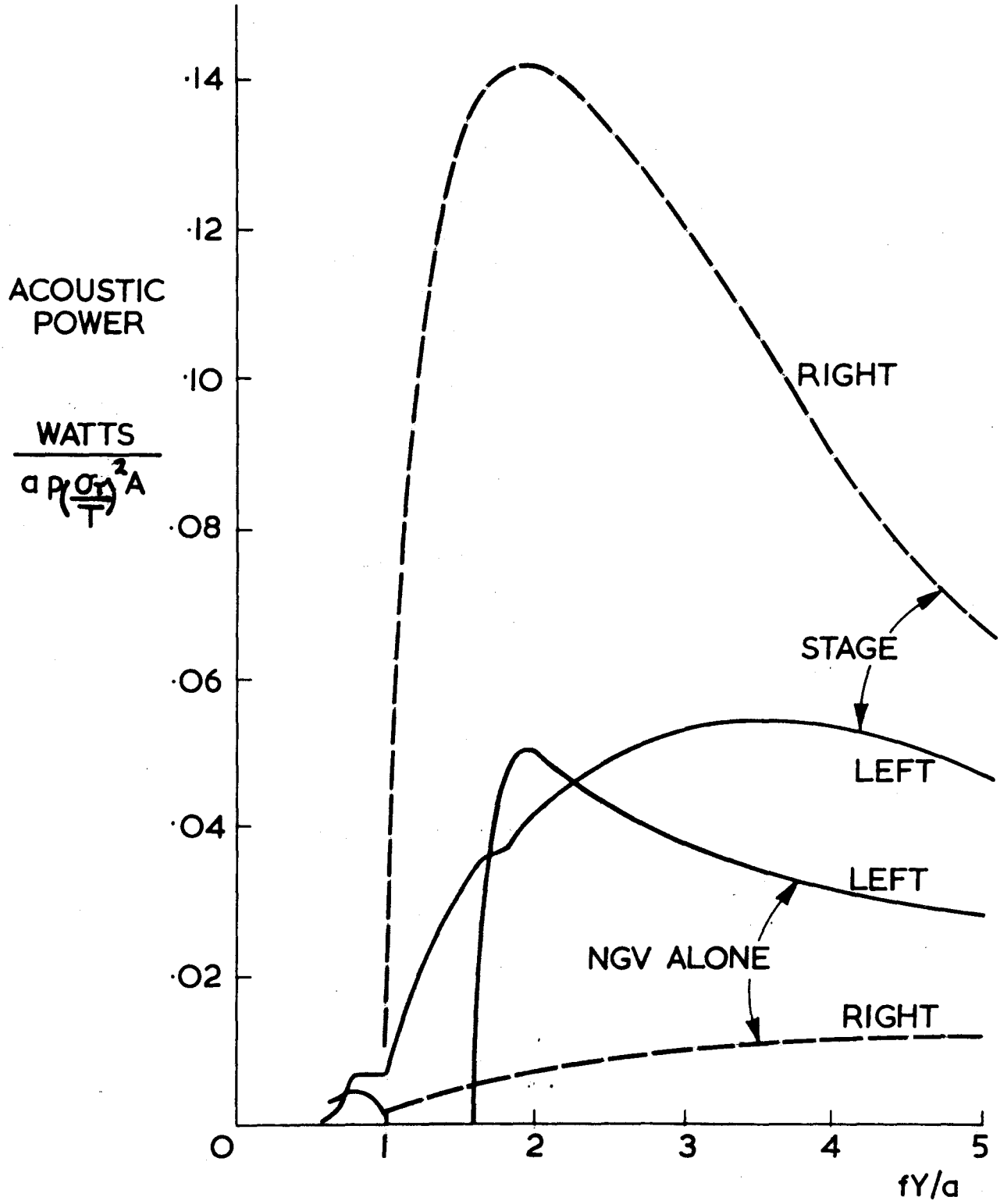

DOWNSTREAM ACOUSTIC POWER DUE TO ENTROPY WAVE INTO ISOLATED TURBINE STAGE AND INTO NGV ALONE

FIG. 10

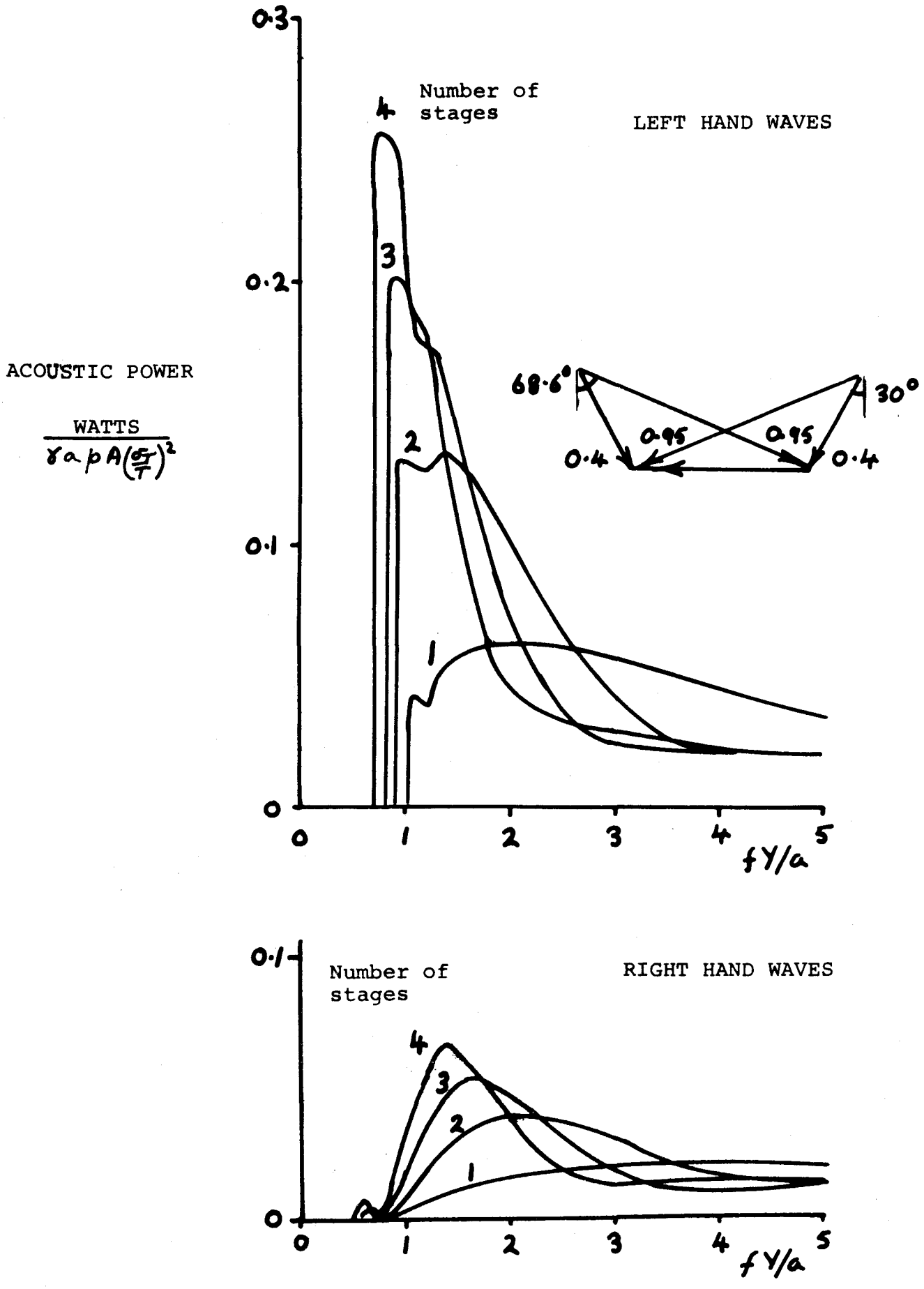

Variation of acoustic power with frequency for repeating turbine stages of 50% reaction Fig. 11